IEEE Access
Multidisciplinary | Rapid Review | Open Access Journal

Received August 16, 2020, accepted August 23, 2020, date of publication August 31, 2020, date of current version September 11, 2020.

Digital Object Identifier 10.1109/ACCESS.2020.3020623

Towards an Adaptive Design of Quality, Productivity and Economic Aspects When Machining AISI 4340 Steel With Wiper Inserts

ADEL TAHA ABBAS[1], MOHAMED ABUBAKR[2], AHMED ELKASEER[3,4], MAGDY M. EL RAYES[1], MONIS LUQMAN MOHAMMED[1], AND HUSSIEN HEGAB[2]

[1]Department of Mechanical Engineering, College of Engineering, King Saud University, Riyadh 11421, Saudi Arabia
[2]Department of Mechanical Design and Production Engineering, Faculty of Engineering, Cairo University, Giza 12613, Egypt
[3]Department of Production Engineering and Mechanical Design, Port Said University, Port Fuad 42526, Egypt
[4]Institute for Automation and Applied Informatics, Karlsruhe Institute of Technology, 76344 Karlsruhe, Germany

Corresponding author: Adel Taha Abbas (aabbas@ksu.edu.sa)

This work was supported by the Deanship of Scientific Research at King Saud University through a research group under Grant RG-1439-020.

ABSTRACT The continuous pursue of sustainable manufacturing is motivating the utilization of new advanced technology, especially for hard to cut materials. In this study, an adaptive approach for optimization of machining process of AISI 4340 using wiper inserts is proposed. This approach is based on advance yet intuitive modeling and optimization techniques. The approach is based on Artificial Neural Network (ANN), Multi-Objective Genetic Algorithm (MOGA), as well as Linear Programming Techniques for Multidimensional Analysis of Preference (LINMAP), for modeling, optimization and multi-criteria decision making respectively. This integrated approach, to best of the authors' knowledge, has been deployed for the first time to adaptively serve different designs of manufacturing processes. Such designs have different orientations, namely cost, quality, productivity, and balanced orientation. The capability of the proposed approach to serving such diverse requirements answers one of the most accelerating demands in the manufacturing community due to the dynamics of the uprising smart production lines. Besides, the proposed approach is presented in a straightforward manner that can be extended easily to other design orientations as well as other engineering applications. Based on the proposed design, a balanced general setting of 197.4 m/min, 0.95 mm, and 0.168 mm/rev was recommended along with other settings for more sophisticated requirements. Confirmatory experiments showed a good agreement (i.e., no more than 7% deviation) with the predicted optimum responses. This shows the validity of the proposed approach as a viable tool for designers to promote holistic and sustainable process design.

INDEX TERMS Adaptive design, artificial neural networks, genetic algorithm, modeling, wiper inserts, turning.

NOMENCLATURE

ANN	Artificial Neural Network.
B	Balanced design.
DOC	Depth of Cut.
EC	Intensive cost-oriented design.
EP	Intensive productivity-oriented design.
EQ	Intensive quality-oriented design.
f	Feed.
GRA	Gray Relation Analysis.
IC	Intensive cost-oriented design.
IP	Intensive productivity-oriented design.
IQ	Intensive quality-oriented design.
LINMAP	Linear Programming Techniques for Multidimensional Analysis of Preference.
MOGA	Multi-Objective Genetic Algorithm.
MRR	Material removal rate.
NSGA	Non-dominated sorting genetic algorithm.
Ra	Average surface roughness.

The associate editor coordinating the review of this manuscript and approving it for publication was Kai Li.

RSM	Response surface method.
USD	United States Dollar.
V_c	Cutting Speed.

I. INTRODUCTION

Owing to the rapidly accelerating global demand for high-quality and sustainable products, scientific and manufacturing communities are now focusing on sustainable machining evaluation and design [1], [2], with particular focus on coming up with innovation and creative solutions in metal cutting technology. Tooling, as an essential aspect of metal cutting, has been a topic of interest when it comes to these solutions. This led to proposing a variety of ideas in the literature, such as tool coating [3], [4], tool texturing [5], [6], and coming up with new tool materials, designs, and geometries [7], [8]. Besides, new cooling strategies have been applied, such as MQL [9], [10] and cryogenic cooling [11], [12]. All these innovative techniques and others are all aiming for the same goal, which is enhancing product quality, improving process economics, and resource utilization while minimizing the negative environmental impact. One of these innovations that stands out is using wiper inserts (i.e., multi radii inserts). These inserts are characterized by a specially engineered nose geometry using more than one radius, as shown in Figure 1. Such geometry can allow a higher production rate while keeping the surface roughness at accepted levels [13]. Additionally, It has been proposed to be an alternative for grinding operation [14] as well as being an effective solution for hard turning (i.e., machining products with a treated surface for hardness improvement) [15], [16]. However, due to its multi radii geometry, it has been recommended that the wiper inserts may suffer from higher cutting forces and energy consumption that may negate the economic gain due to the higher operating cost. These potential conflicting responses are the reasons why multi-objective optimization approach is imperative for a successful utilization of the wiper inserts. This has motivated a lot of effort among scholars to optimize the wiper insets based turning process.

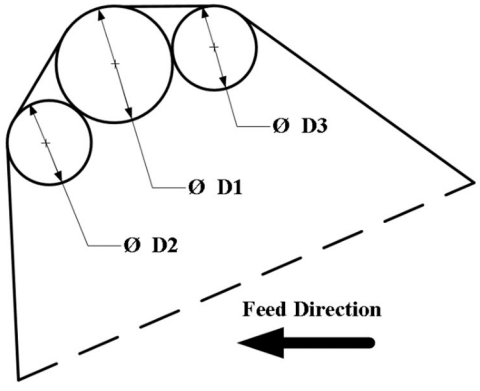

FIGURE 1. Wiper insert geometry.

Elbah *et al.* [17] utilized the response surface method (RSM) and desirability function approach to find the optimal turning parameters of AISI 4140. This is to find cutting velocity (V_c), depth of cut (DOC), and feed (f) that minimizes the three components of surface roughness R_a R_Z and R_t while using wiper insert. Paiva *et al.* [18] used principal component analysis and multivariate mean square error to find out V_c, DOC, and f that minimize five different surface components while turning AISI 52100 hardened steel using wiper inserts. Venkata Subbaiah *et al.* [19] performed multi-objective optimization for turning AISI 4340 using wiper inserts. Desirability function with equal weights based on RSM was used to find out machining parameters (i.e., V_c, DOC, and f) which minimize surface roughness, cutting forces, and tool wear, while maximizing material removal rate. Gaitonde *et al.* [20] utilized an artificial neural network (ANN) to investigate the turning performance of AISI D2 cold work tool steel using wiper and conventional insert. Using the ANN models, plots of different response surfaces were generated for specific cutting force, surface roughness, and tool wear while varying Vc, DOC, inset type, and machining time. By using these plots, machining settings optimizing each response separately was attained (single-objective optimization). Dabade [21] used gray relation analysis (GRA) to optimize cutting forces, surface roughness, and residual stress while machining Al/SiCp composite. Based on equal weight per response, optimum nose radius, f, DOC, and Vc were evaluated. Gray Relation Analysis GRA with equal weights were used to optimize R_a, cutting forces, and hardness while turning AISI 316L and 304L by Basmaci and Ay [22] and Ay [23] respectively. They compared conventional and wiper tools, as well as MQL and flood coolant under different feed rates and cutting speeds.

Venkata Subbaiah *et al.* [24] used grey relational analysis (GRA) to optimize AISI 4340 steel while using both conventional and wiper inserts. Surface roughness and MRR were taken as responses with equal importance while investigating the effect of DOC, f, and Vc as control parameters. Camppos *et al.* [25] utilized principal component analysis (PCA); multivariate mean square error (MMSE), GA, and RSM to model and optimize the turning process of AISI 512100 steel using wiper inserts. PCA was used to reduce tool life, cutting time, total turning cycle time processing cost per piece Ra and Rt into three principal components. Later these principle components were all assigned equal weights during the MMSE formulation. The f, DOC, and Vc were considered as control parameters during the optimization process.

Based on the available information in the open literature for wiper insert and other machining applications [26]–[28], intensive efforts have been made in order to address the optimization of conflicting machining responses. However, none of them provided any sort of adaptive approach which is able to offer different solutions for different designs' orientations of the same process. In other words, no work has utilized the posterior preference articulation approach (PPAA), such as the one proposed in the current study. The main principle of PPAA, as the name implies in "posterior," is that the designer preferences are only applied after obtaining the

Pareto front [29]. This is particularly attractive in problems where finding out the designer's preference is difficult before examining the trade-off between different responses [30]. The PPAA was adopted in a very limited number of studies related to the current application of interest. Pytlak [31] adopted the PPAA approach to optimize the production cost, process time, and cutting force during turning 18HGT steel using CBN wiper insert. The feed, depth of cut, and cutting velocity were considered as control parameters. Using empirical models, the relations between the control parameters and responses were established. The author investigated two approaches (i.e., weighted objective and modified distance method) to compute the Pareto front. Afterwards, according to the PPAA principle, a hierarchical optimization method based on a single weighting case (i.e. single design preference) was performed to select the final solution from the pre-evaluated Pareto front. To the best of the authors' knowledge, no other studies have provided such an adaptive posterior preference articulation approach in this particular application, even though it is proven effective in other applications [32], [33].

In the current study, a new progress has been made to fill this gap. The proposed approach is flexible enough not only to satisfy dynamic changes for the process requirements, but also it is applicable for different applications. For example, a particular setting may be capable of producing very high-quality products but at the expense of high cutting speed (i.e., high power and cost) and at very low productivity.

This solution may be attractive in a process designed for precision machining. However, it is not in other cases where there is no such tight constrain on quality. In fact, such settings will represent an unjustified economic burden on the process. This is why the designer should have handy procedures to tune the process design parameters to meet different needs. This is especially important due to the new production line dynamics imposed as a sequence of the new era of sustainable smart customer-driven manufacturing [34]. In this new concept, the product line should always be dynamic and cable of keeping up with the rapid change in the required product specifications and even generate different products from the same production line [35].

For that reason, it is imperative to integrate adaptive process design approaches, such as the proposed one in this study, with advanced machining technologies, like the innovative wiper insert design, to promote sustainability in the era of smart manufacturing.

Following this introduction, the remaining of this article is outlined as follows. Firstly, in the methodology section, the proposed intuitive framework will be outlined for the wiper inset based machining, as shown in Figure 2. This started with data collection, where the experiment design and procedures are outlined. These two are considered as application identifiers to the proposed algorithm and can be adjusted for different applications. Afterward, these data are fed to a modeling algorithm to produce the necessary mathematical model for the optimization technique. It should be stated that in this study, artificial neural network modeling was used with genetic algorithm optimization, and both showed adequate performance through validation. However, the followed framework is flexible, allowing for different modeling and optimization techniques depending on the data complexity. To check the independency of the obtained solution from the probabilistic features of both the ANN model (i.e., data set randomization, initial weights, and biases) as well as the MOGA operators (i.e., initial population, mutation, cross over and tournament selection), the whole approach in Figure 2 was repeated 3 times per each design criteria listed in Table 3, and the difference between the final selected settings was found insignificant. Finally, the core of the adaptive design methodology is implemented by using a variety of weighting strategies for a different design using Linear Programming Techniques for Multidimensional Analysis of Preference (LINMAP). Each of these steps will be discussed while focusing on the means to adopt this approach for different problems. Afterward, an intensive discussion will be provided to show the superiority and trades-off between the different proposed designs.

II. EXPERIMENTATIONS AND METHODS

A. EXPERIMENTATION

In this study, AISI 4340 steel test specimen was machined under flood water-miscible cooling on the EMCO concept turning machine shown in Figure 3. The test specimen was prepared, as shown in Figure 3 so that a single bar can be used for four experimental runs. For each run, only 12 mm length is machined, followed by 10 mm of clearance. Afterward, 8 mm of the 12 mm machined length is used for the surface roughness measurements. During the machining process, power consumption was recorded through power clamp meters (Tactix 403057). The full details of the materials and tools used are illustrated in Table 1. A total of 30 experimental runs were performed covering a cutting speed (Vc) range from 150 to 200 m/min, depth of cut (DOC) of 0.5 to 1 mm, and feed (f) from 0.05 to 0.25 mm/rev. The design of the experiment was based on mixed levels general full factorial array with 30 runs, as shown in Table 2. In order to solve the optimization problem, all responses should be represented by a mathematical formula which is continuous in the entire search domain. For the material removal rate, this is attainable by equation (1). However, for surface roughness and power consumption, such equations were established using the ANN modeling, as discussed in the next section. Finally, equation (2) was utilized to represent the total machining cost. It includes a breakdown of the different costs as follows: machine operation and depression, tool wear and cooling cost of 1.67, 0.25, and 0.032 [USD/min], respectively, as well as energy cost 0.032 [USD/min/kW].

$$MRR = V_c * DOC * f \tag{1}$$

$$\begin{aligned} C(f, V_c, DOC) = {} & machining\ time \\ & * [1.67 + 0.25 + 0.032 + 0.0013] \\ & * P(f, V_c, DOC) \end{aligned} \tag{2}$$

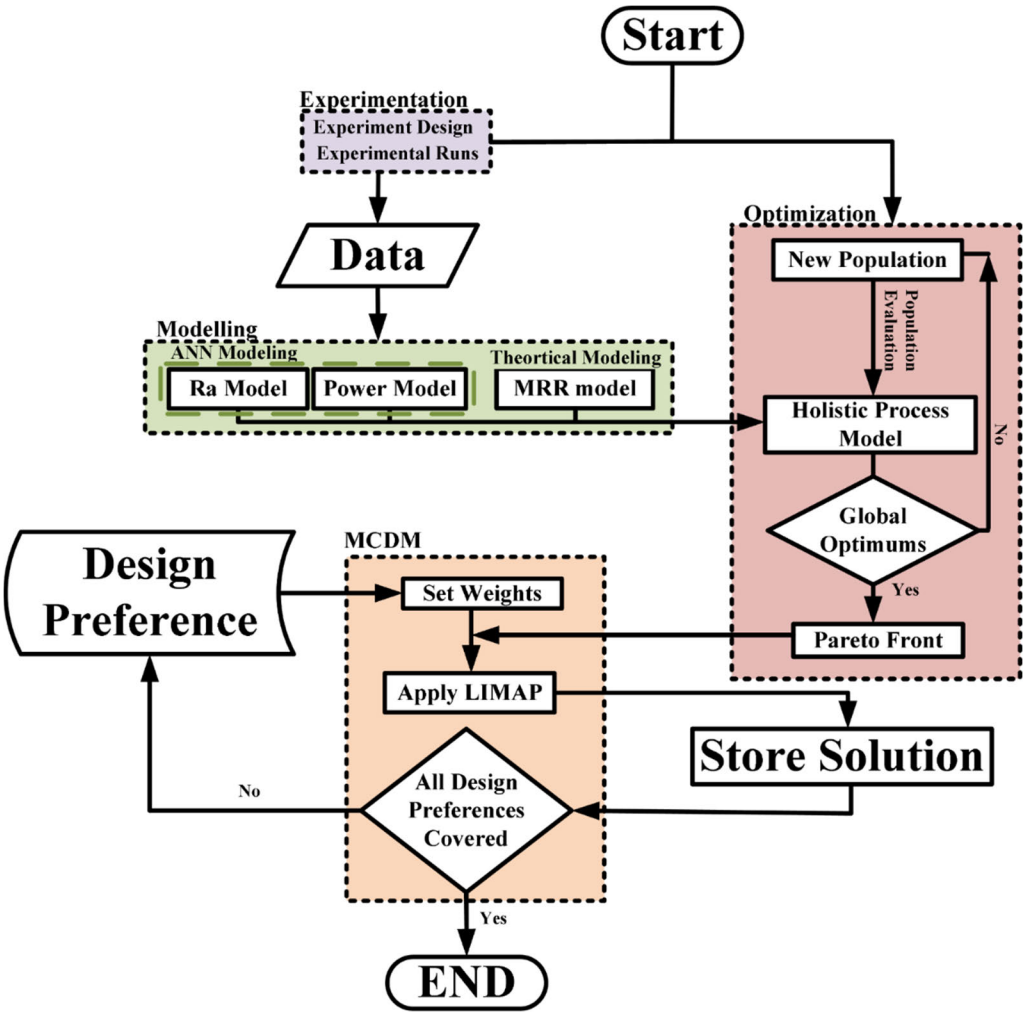

FIGURE 2. Problem tackling approach for adaptive solutions.

where C is the total cost, and P Represents the consumed power during the machining process in kW predicted from the developed ANN model, as shown in the next section.

III. DATA-DRIVEN MODELS

In order to optimize the machining process settings, accurate closed-form mathematical models, correlating the response variables to the corresponding tuned parameters, are required. This mathematical model is a vital tool to allow utilizing a robust optimization algorithm, as described in the next section. In the current study, the artificial neural network was utilized to construct two models, the surface roughness model, and the power model. The experimental data was randomized and split into three subsets. The first subset includes 15% of the entire data set that are excluded from the training process, while the rest is used during the training and validation steps. Even though the data was randomized, the accuracy of the model can be sensitive to the distribution of the rest of the 85% of the data among training and validation. This is why, in this study, k fold cross-validation was used to eliminate this sensitivity. Cross-validation was utilized to prevent overfitting of the ANN model. During the cross-validation process, the number of folds was varied from 1 to 5, and the closest fold to the mean was taken as the final fold [36], [37]. The training is based on the backpropagation technique to set the optimum weights of the feed-forward neural network [38], [39]. Deciding the ANN topology is another critical step to avoid over and underfitting the data. In this study, the sigmoid function was selected as the activation function, and different ANN topologies were tested for the two models. As shown in Figure 4(a & b), shallow ANN (one middle layer) with three neurons showed the lowest variance (RMSE) of 0.074 μm and 0.044 kW for surface roughness and power models. For this reason, this particular ANN topology is used during the rest of the analysis. Figure 4(c & d) shows the goodness of fit for both models. In general, models show a good fit with R^2 no less than 0.95 for both training and test data. In fact, these figures show that these two models provide a higher R^2 for the testing data set compared to the training one. This is a desirable feature

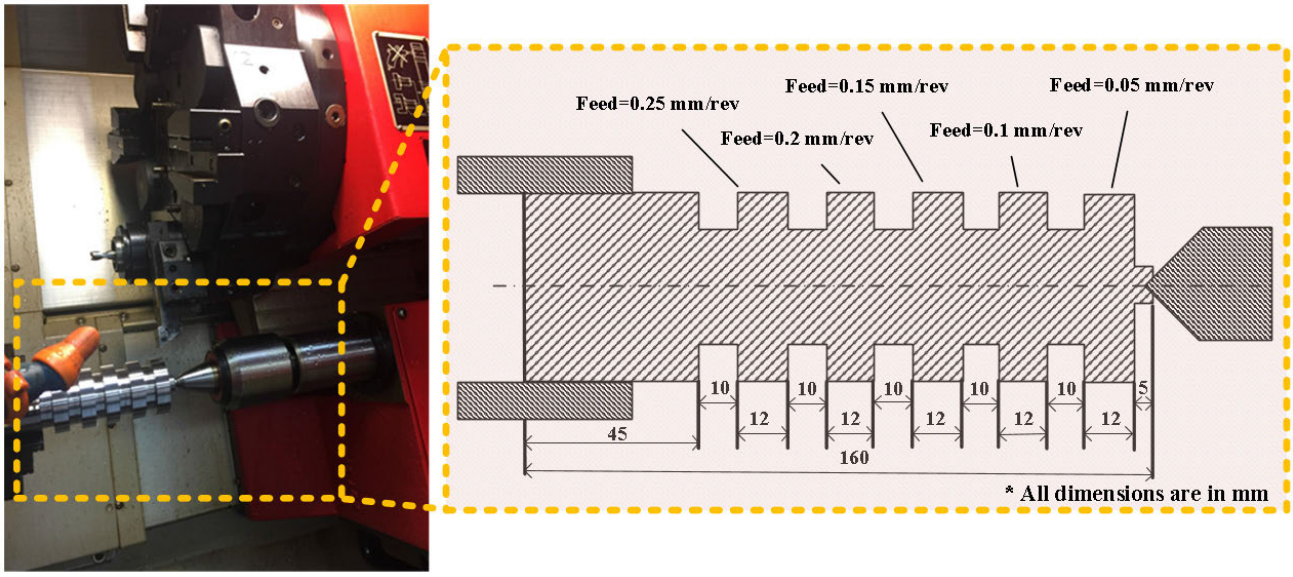

FIGURE 3. Test rig for machining and specimen.

TABLE 1. Tools and materials.

Item	Description
Turning center lathe	EMCO Concept Turn 45 CNC lathe (EMCO, Salzburg, Austria)
Bars material	50 mm diamater 130 mm long AISI 4340 steel bars with a chemical composition of Ni: 2.5%, Cr: 0.9%, Mn: 0.50%, Mo: 0.41%, C: 0.40%, Si: 0.12%, V: 0.09% by weight and Fe Balance
Inserts	Wiper (DCMX 11 T304-WF GC4325) Nose radius=0.4 mm, 55° cutting edge angle,7° clearance angle and a positive rake angle of 6°
Tool holder	SDJCL 2020K11
Coolant	ECO-COOL-MK-3 cutting coolant fluid, diluted in distilled water (1 Vol. of ECO-COOL-MK-3 to 5 Vol. of distilled water, Saudi Petroleum company, Jeddah, Saudi Arabia).
Surface roughness tester	TESA (Switzerland) surface roughness tester, type "Rugosurf 130 90-G" (8 mm cut-of-length)
Power logger	Tactix 403057

since these models will be utilized as an objective function for the optimization algorithm. And the prediction performance is a critical aspect for such models. This is because there is no guarantee that the evaluated points during optimization algorithm fails within the training data set.

A. OPTIMIZATION TECHNIQUE

The optimization problem in this study is solved by utilizing the (MOGA) multi-objective genetic algorithm. MOGA is one of the most commonly used optimization techniques in manufacturing applications [40], [41]. In this study, MOGA is used to optimize all three objectives (roughness, MRR, and cost), as shown in equation 3.

$$\begin{cases} Minimize\ \text{Ra} = f_1(V_c, DOC, f) \\ Maximize\ \text{MRR} = f_2(V_c, DOC, f) \\ Minimize\ \text{Cost} = f_1(V_c, DOC, f) \\ Subject\ to: \\ 150 \leq V_c \leq 200 m/min \\ 0.5 \leq \text{DOC} \leq 1 mm \\ 0.05 \leq I \leq 0.25 mm/rev \end{cases} \quad (3)$$

TABLE 2. Experiemetal runs.

Test #	V_c [m/min]	DOC [mm]	f [mm/rev]	Ra [μm]	Power [kW]	MRR [mm^3/min]
L1	150	0.50	0.05	0.248	2.90	3750
L2			0.10	0.320	3.13	7500
L3			0.15	0.441	3.33	11250
L4			0.20	0.803	3.60	15000
L5			0.25	1.329	3.80	18750
L6	150	0.75	0.05	0.224	3.00	5625
L7			0.10	0.329	3.20	11250
L8			0.15	0.414	3.53	16875
L9			0.20	0.995	3.80	22500
L10			0.25	1.564	4.07	28125
L11	150	1.0	0.05	0.256	3.13	7500
L12			0.10	0.369	3.40	15000
L13			0.15	0.503	3.67	22500
L14			0.20	0.955	3.93	30000
L15			0.25	1.757	4.20	37500
L16	200	0.5	0.05	0.172	3.20	5000
L17			0.10	0.366	3.53	10000
L18			0.15	0.548	3.80	15000
L19			0.20	1.241	4.27	20000
L20			0.25	1.899	4.56	25000
L21	200	0.75	0.05	0.294	3.47	7500
L22			0.10	0.342	3.80	15000
L23			0.15	0.496	4.10	22500
L24			0.20	0.524	4.57	30000
L25			0.25	1.362	4.90	37500
L26	200	1.0	0.05	0.249	3.53	10000
L27			0.10	0.290	3.87	20000
L28			0.15	0.536	4.20	30000
L29			0.20	0.673	4.67	40000
L30			0.25	1.236	5.00	50,000

The MOGA algorithm used in this study is the basic real coded genetic algorithm (GA) equipped with a non-dominated sorting NSGA-II algorithm. The GA algorithm is a powerful single objective optimization tool. It mimics the natural selection and survival of the fittest. An initial population whose size is predefined, based on hypervolume, as will be discussed later, is compared together based on the objective function (i.e., fitness value). The fitter the solution is, the higher its probability of survival to next-generation (roulette wheel tournament). Those who have survived will also have a higher probability of having a chance for reproduction based on using mutation (i.e., exploration) and cross over (i.e., exploitation) operators. These processes are continued to the predefined number of generations, chosen based on hypervolume, as discussed later [42]. When this criterion is satisfied, the optimum solution can be easily identified. However, the above-mentioned algorithm works very well for a single objective; it is not applicable in the multi-objective optimization. This is because of the contradicting nature of the objectives of interest. Thus, solutions that are achieving one objective are usually failing the others. This intrinsic feature in multi-objective optimization is the reason behind replacing the concept of the best individual solution in GA by the set of non-dominated solutions in MOGA using NSGA-II algorithm [42], [43].

The selection of hyperparameter while setting the MOGA is very critical. In this study, a uniform initialization function, size of two tournament selection, and 0.8 crossover fraction were used. A low mutation rate of 0.01 was selected to avoid missing the optimum value when the current result is in the vicinity of the global optimum solution. On the other hand, the number of generation and the particle population size, as they are susceptible to each particular problem nature, was tuned using the hypervolume technique. Maximizing the hypervolume is considered as an indication of both closeness to the true Pareto (accuracy) and diversity [44], [45].

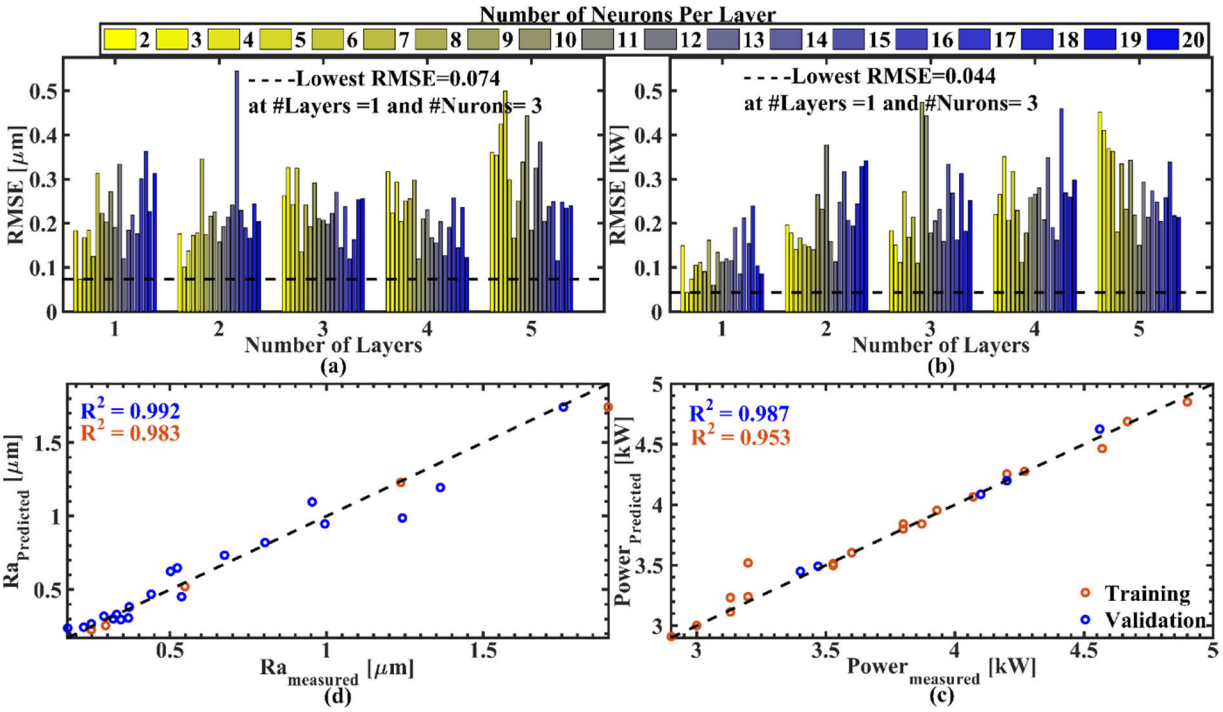

FIGURE 4. (a & b) performance of different tested ANN topology for Ra and Power, respectively, (c & d) Scatter plots showing the goodness of fit of the two selected ANN models for Ra and Power, respectively.

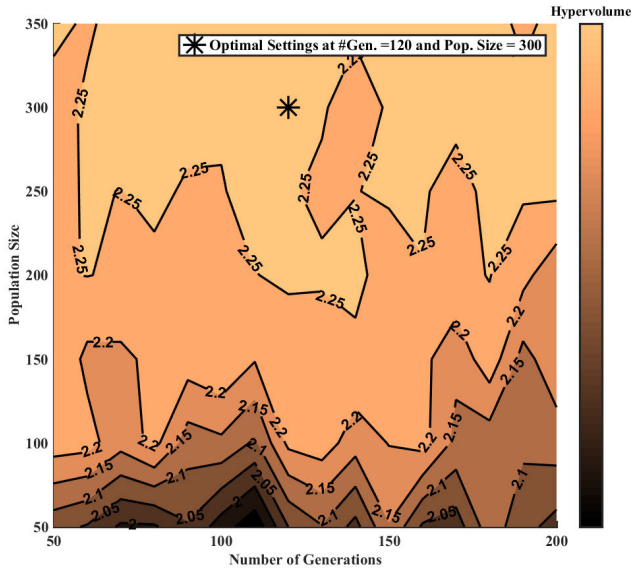

FIGURE 5. Illustration of hypervolume optimal settings.

Based on the hypervolume maximization using exhaustive grid research shown in Figure 5, a population of 120 points and 130 generations were utilized in MOGA setup.

B. DECISION-MAKING TECHNIQUE

The selection of the final point from the computed Pareto front is challenging. The reason for that is the fact that each solution in the Pareto front is not dominated by any other solution. This is why switching between any two solutions on the Pareto front will always be associated with improving one objective at the expense of the others. For this reason, in the core of this adaptive design comes the Linear Programming Techniques for Multidimensional Analysis of Preference (LINMAP), which is a Multi-Criterion Decision-Making Algorithm (MCDMA). In this design, it is utilized to transform the vast Pareto solutions into a single solution based on the particular design criteria (i.e., weights assigned for each objective). In LINMAP, the first step is the Euclidian non-dimensionalization. It is performed in order to put aside any fake influence of the diverse ranges and magnitudes of the objectives of interest [46].

$$F_{xy}^{n} = \frac{W_x F_{xy}}{\sum_{y=1}^{m} F_{xy}} \tag{4}$$

where x is an objective index ($x = 1$: Ra; $x = 2$: MRR; and $x = 3$: Cost), y is a particular Pareto solution and m is the number of optimization objectives. F_{xy}^{n} is the normalized and scaled version for the original objective x of the yth solution (F_{xy}). The weight (W) is the core of the adaptive design. Based on its value, the design dependence on different objectives can be altered from 0% (i.e., independent) to 100% (i.e., solely dependent) on this particular objective. Afterward, the distances between the point under evaluation and the utopian point are evaluated. The utopian point is an imaginary point at which all objectives are at the optimum level (minimum if minimization and maximum otherwise).

TABLE 3. Weights used for different designs.

	Ra [μm]	MRR [mm^3/min]	Power [kW]
Balanced (B)	0.33	0.33	0.33
Extensive Quality (EQ)	0.6	0.2	0.2
Extensive Productivity (EP)	0.2	0.6	0.2
Extensive Economy (EE)	0.2	0.6	0.2
Intensive Quality (IQ)	1	0	0
Intensive Productivity (IP)	0	1	0
Intensive Cost (IC)	0	0	1

This distance is calculated as follows:

$$d_y^+ = \sqrt{\left(\sum_{x=1}^{t}(F_{xy}^n - F_{xutopian}^n)\right)^2} \quad (5)$$

The lower the distance, the better that point fits this particular design. In this approach, the closest point to the utopian (smallest d_y^+) is ranked first, and the same ranking criteria is used to rank the rest of the Pareto front solutions if needed.

C. ADAPTIVE WEIGHTING

The core of this study is providing intuitive straight forward procedures that can be tailored for different applications. Besides, it should be adaptive enough to provide the designer with flexible alternative designs based on different criteria. Without the proposed adaptive design, the multi-objective optimization will lead to a set of solutions (i.e., Pareto front) that none of its individual is the best choice in all objectives. The selection from these points is a challenging task. This is due to the fact that preferring any individual solution over another one will lead to a penalty on some of the objectives while improving the others. This is why, in this study, different weighting criteria shown in Table 3 are implemented while applying LINMAP to improve the efficiency of this final selection process. It worth mentioning that this will not eliminate the penalty mentioned earlier; however, it will localize the damage in the objective which the designer is least interested in. For example, consider a rough turning process where the main concern is to maximize the MRR, the extensive productivity design in Table 3 will be an excellent choice to get the machining setting. Besides, a more aggressive setting can be implemented obtained by increasing the MRR weight to unity, as shown in Table 3, for the intensive productivity design. The difference between aggressive and intensive design is similar to the difference between single and multi-objective design. In other words, in the intensive designs, all the focus is directed to one objective regardless of the others. It is even possible to extend the outlined procedures in Figure 2 beyond the suggested design values in Table 4. In fact, the procedures are represented in this study in an intuitive form that can be extended to handle any process design. Besides, Table 4 is just an example of four designs re-occurring in the manufacturing application altering the focus between process cost and productivity as well as product quality.

IV. RESULTS AND DISCUSSION

In this section, the results obtained from the proposed adaptive approach are discussed based on Table 3. The final Pareto front set of solutions obtained from MOGA optimization is shown in Table 4. For each solution, the machining parameters (f, DOC, and V_c), as well as the corresponding

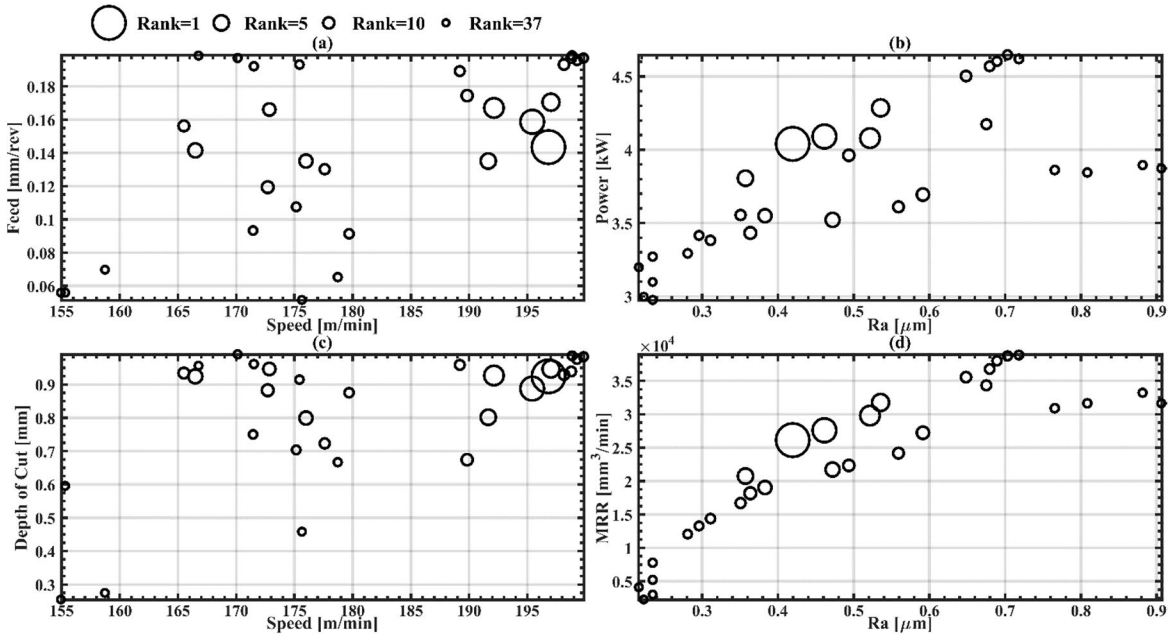

FIGURE 6. Pareto front, ranked using LINMAP for a balanced design.

TABLE 4. Ranked Pareto solutions for all designs.

Vc	DOC	f	Ra	MRR	Power	Ranks						
[m/min]	[mm]	[mm/rev]	[µm]	[mm^3/min]	[kW]	B	EQ	EP	EC	IQ	IP	IC
196.8	**0.93**	**0.14**	**0.419**	**26131.6**	**4.04**	**1**	9	15	9	13	15	21
195.4	0.89	0.16	0.461	27583.7	4.09	2	14	12	12	14	13	23
192.2	0.93	0.17	0.521	29806.6	4.08	3	17	8	13	17	12	22
197.0	0.95	0.17	0.535	31799.2	4.28	4	18	7	15	18	8	25
191.6	**0.80**	**0.13**	**0.358**	**20747.8**	**3.80**	5	**1**	19	5	10	19	15
166.5	0.92	0.14	0.472	21767.6	3.52	6	15	18	2	15	18	10
176.0	0.80	0.13	0.383	18989.1	3.55	7	8	20	3	12	20	11
172.8	0.95	0.17	0.591	27172.6	3.70	8	20	13	7	20	14	14
172.7	**0.88**	**0.12**	**0.364**	**18209.7**	**3.43**	9	6	21	**1**	11	21	9
189.8	0.67	0.17	0.494	22321.4	3.96	10	16	17	14	16	17	20
165.5	0.93	0.16	0.559	24151.0	3.61	11	19	16	4	19	16	13
198.1	**0.93**	**0.19**	**0.649**	**35503.5**	**4.50**	12	21	**1**	25	21	5	26
177.6	0.72	0.13	0.351	16714.7	3.55	13	5	22	6	9	22	12
189.2	0.96	0.19	0.675	34299.4	4.18	14	22	6	18	22	6	24
198.8	0.94	0.20	0.680	36768.1	4.57	15	23	3	27	23	4	27
179.7	0.88	0.09	0.311	14406.2	3.38	16	2	23	8	8	23	7
199.3	0.97	0.20	0.689	37964.4	4.60	17	24	2	28	24	3	28
199.9	0.98	0.20	0.703	38757.8	4.65	18	25	4	29	25	2	30
175.1	0.70	0.11	0.296	13282.1	3.41	19	3	24	10	7	24	8
199.8	**0.99**	**0.20**	**0.718**	**38916.1**	**4.62**	20	26	5	30	26	**1**	29
171.5	0.75	0.09	0.280	12018.4	3.30	21	4	25	11	6	25	6
175.4	0.91	0.19	0.765	30954.6	3.86	22	27	9	17	27	11	17
171.5	0.96	0.19	0.808	31671.6	3.84	23	28	10	20	28	10	16
178.7	0.67	0.07	0.235	7777.8	3.27	24	7	26	16	4	26	5
170.1	0.99	0.20	0.881	33167.2	3.89	25	29	11	24	29	7	19
155.3	**0.60**	**0.06**	**0.235**	**5187.8**	**2.97**	26	10	27	19	5	27	**1**
166.8	0.96	0.20	0.907	31678.1	3.87	27	30	14	26	30	9	18
175.7	**0.46**	**0.05**	**0.216**	**4145.9**	**3.20**	28	11	28	21	**1**	28	4
158.7	0.27	0.07	0.234	3034.7	3.10	29	12	29	22	3	29	3
155.0	0.25	0.06	0.223	2210.2	3.00	30	13	30	23	2	30	2

machining responses (Ra, MRR, and Cost), are outlined. Besides, these solutions are also ranked based on different designs in Table 3, and the highest rank solution for each design is bolded for convenience. Based on Table 4, the conventional Pareto front can be upgraded, as shown in Figure 6, for the balanced (B) case. The figure shows the final Pareto front in two different domains, the machining parameters domain in Figure 6 (a & c) and the corresponding machining responses in Figure 6(b & d). In addition, Figure 6 shows the ranks by varying the circle radius. The fittest point for the balanced design is assigned with the biggest radius.

Although, Figure 6 is limited to a balanced case. Similar figures can be generated for the other designs based on Table 4. Figure 6 shows that for the balanced design, the highest-ranked solutions are clustered at the high cutting speed (195 m/min and higher) and high depth of cut (1 mm) relative to other Pareto solutions, as shown in the top right corner in Figure 6 (c). Additionally, in general, moderate feeds around 0.14 mm/rev shows higher ranks, as shown in Figure 6 (a). Moreover, since this design is compromising between all the responses, Figure 6 (b & d) are showing that the highly ranked solution is in the middle

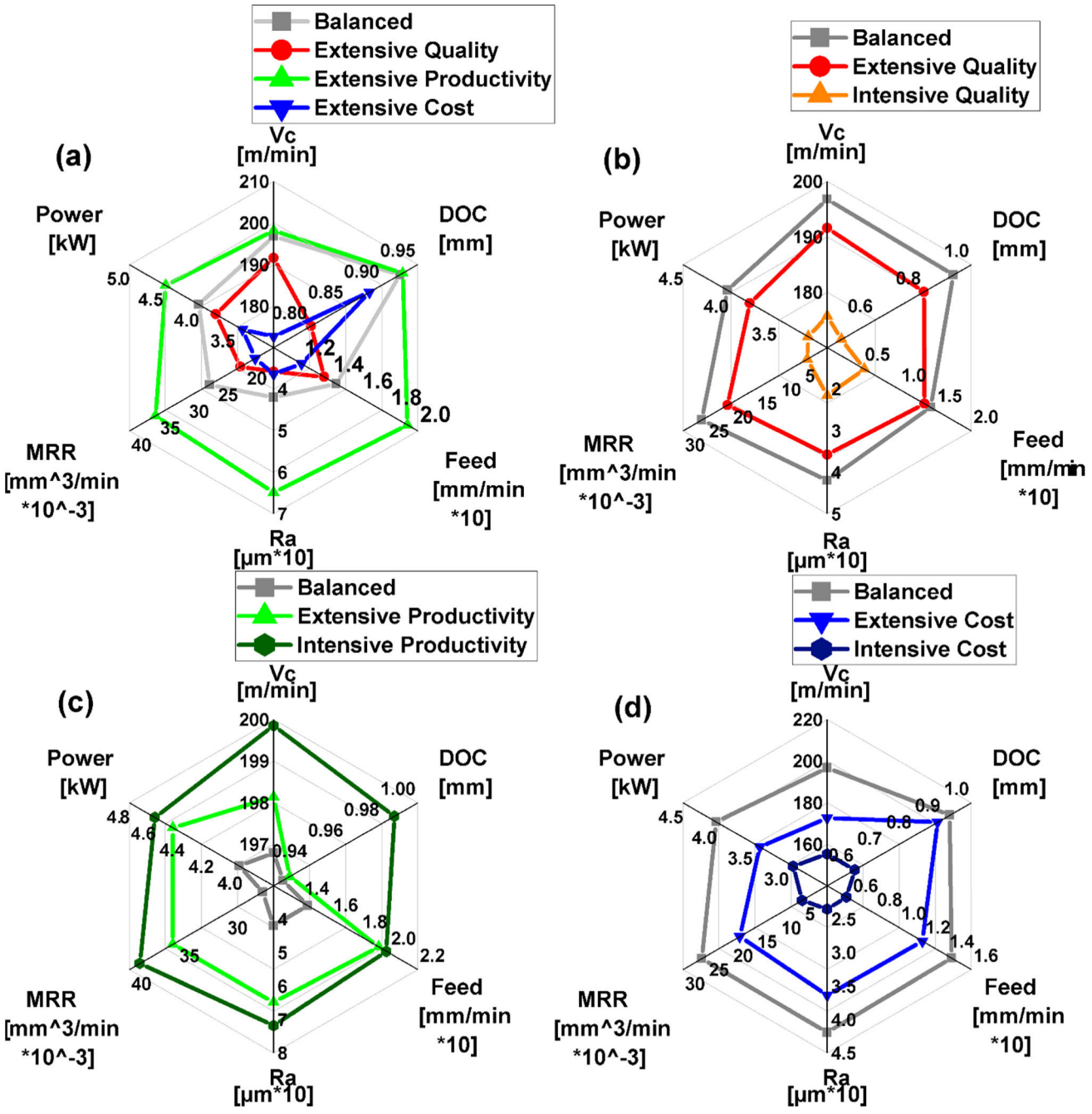

FIGURE 7. Key solutions from the adaptive design.

of all responses (i.e., power, Ra, as well as MRR). These particular settings are attractive for most basic operation needs, especially if no sophisticated constraints are imposed on the process performance. However, such general basic requirements are not guaranteed for all applications at all the time. This is why numerous alternatives were proposed in the current study, as shown in Figure 7. This shows an example of the proposed adaptive approach capabilities. Figure 7 represents a comparison between all seven designs proposed in Table 3.

The balanced one, as discussed earlier, has no preference in preferring one aspect over the others. However, on the other hand, each of the other extensive designs focuses on a specific aspect while at the same time, takes the other aspects into consideration. On the other extreme comes the intensive designs, as shown in Figure 7 (b to d). In these designs, all the attention is paid to one aspect of the machining responses regardless of the others. In Figure 7 (a), it is evident that the machining responses considered in this study are conflicting and cannot be all optimized simultaneously. For example,

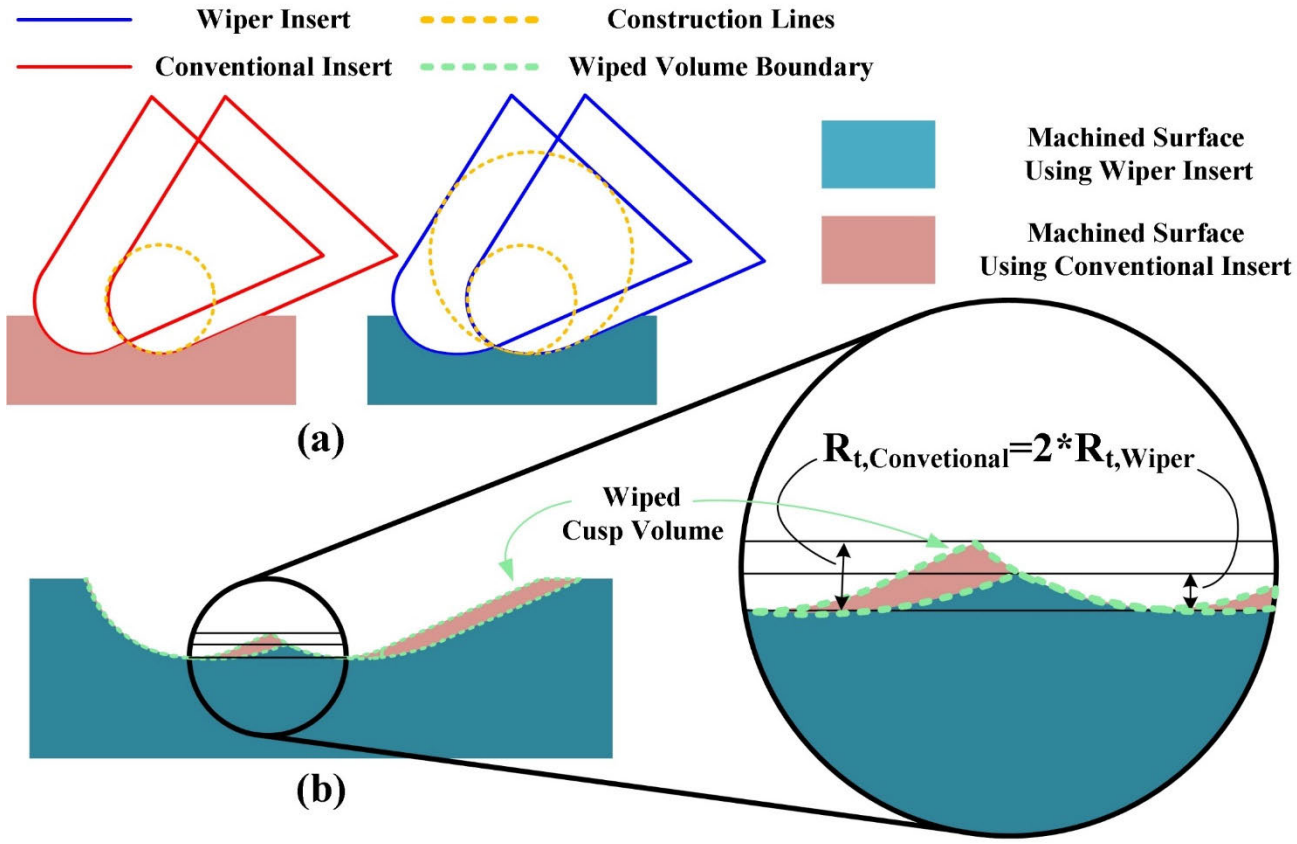

FIGURE 8. (a) Conventional and wiper inserts engagement with the workpiece, (b) wiped asperities and surface profile generated by wiper inserts.

the extensive quality case (EQ), the surface roughness, shows the lowest value (0.35 μm); however, this comes at the expense of productivity in terms of MRR (2074.8 mm^3/min). This value is 41.5% lower than the MRR obtained for the extensive productivity case of 3550.3 mm^3/min. This shows that there is no single solution that will be globally accepted for all operations. For example, for precision machining or finish machining process, the intensive quality case, shown in Figure 7 (b), will be favorable even though it will bring the productivity (MRR) nearly to half its value compared to the extensive quality case which is still a quality-oriented case. However, this may be justified for finishing or precise machining since the Ra has improved by 40%.

It is important to notice that the proposed design is flexible since the designer is not obligated to choose between these two extremes. This is due to the fact that Table 4 provides more modulating, smooth transitional solutions between them. Figure 7 (c & d) extends the aforementioned decisions to productivity and economics design. The intensive production design is a good option for a rough machining process while the cost design-intensive is focused on low energy consumption, which is critical when only smaller machines are available or when the power rating is high (i.e., during peak electricity demand hours). Comparing the balanced design and extensive production design gives insights about the great advantage of wiper inserts. These two designs are very close in terms of cutting speed as well as the depth of cut with values around 197 m/min and 0.93 mm, respectively. However, the main difference between these two settings is in the feed rate, which has increased from 0.14 to 0.19 mm/rev, respectively (i.e., 1.36 folds increase). Correspondingly the MRR and Ra have increased by 1.36 and 1.55 folds, respectively. Although such a trade-off between productivity and quality in these two designs is expected, using the wiper inserts led to damping the quality sacrifice.

To prove this, consider the rule that for conventional machining, the Ra is directly proportional to the square of the feed rate [47]. Based on this rule, the 1.36-fold increase in the feed should have led to about 1.85 folds increase in the Ra instead of the recorded 1.55 folds. This proves the capability of the wiper inserts to handle higher feeds, which is contributed to its unique multi-radii geometry. The multi-radii nose of the wiper inserts leads to a larger engagement area between the workpiece and the tool. Such extended engagement is a feature that the conventional insert lacks, as shown in Figure 8 (a). This extended engagement will lead to different effects exclusive to the wiper inserts. The first is a wiping effect by the secondary nose to the cusp region created by the first nose, which shortens asperities peaks [48], as shown in Figure 8 (b). The second effect

is the higher cutting temperature corresponding to higher friction and heat generation [49]. This is why it is expected to have a considerable increase in the cutting forces and power associated with the usage of wiper inserts [50]. Even though the cutting forces increase, the wiper inserts are still known to have longer tool life [49], [51]. This is explained by the better distribution of this force on the extended engaged cutting length, which can improve the tool life up to 20% [52]. However, this extended contact decreases force; it can adversely induce chatter in the tool holder and machine [53]. This is because the extended length is considered as a form of extra tool-workpiece engagement, which is known to enhance chattering. For this reason, extra precautions (i.e., using vibration damper or increase machine and tool holder rigidity) may be required while using wiper inserts [47].

These diverse consequences of using wiper inserts are the reason why applying this proposed holistic and adaptive process design is essential. This is because that approach is a handy tool to deal with the contradicting machining responses at different machining settings, which is an extremely challenging task, particularly for a dynamic process. The proposed approach in this study is not only capable of coping with this and optimize the utilization of the wiper inserts but is also applicable to different innovative machining technologies as well as other applications. To further validate the proposed procedures, four confirmatory experiments were conducted according to the parameters of the top four ranked solutions from selected designs. As shown in Table 5, the experimental results agree with the predicted ones. No deviation of more than 7% was found for any of the measured parameters.

TABLE 5. Confirmatory runs.

	Case	B	EQ	EP	EC
Ra [μm]	Predicted	0.419	0.358	0.649	0.364
	Experimental	0.421	0.344	0.621	0.389
	Deviation (%)	**-0.48**	**4.07**	**4.51**	**-6.43**
Power [kW]	Predicted	4.04	3.80	4.50	3.43
	Experimental	3.97	3.87	4.61	3.287
	Deviation (%)	**1.76**	**-1.81**	**-2.39**	**4.35**

V. CONCLUSION AND FUTURE WORK

In this study, the machining parameters of AISI 4340 using wiper inserts were optimized according to different seven standard manufacturing design criteria. To attain such a task, an adaptive framework was developed, which involved data-driven modeling as well as evolutionary and multi-criteria-based optimization. The data-driven modeling was performed using Artificial Neural Network (ANN). This process involved ANN topology tuning and cross-validation to assure coming up with a robust and generalized model. Such models were used to represent the surface roughness, cost, and power. In the optimization stage, a genetic algorithm was tuned using hypervolume and integrated with Linear Programming Techniques for Multidimensional Analysis of Preference (LINMAP) to complete the novel proposed adaptive approach. Based on this approach, different solutions have been proposed for several sophisticated requirements. Besides, one of these solutions has been formulated to serve the most common manufacturing application. This is referred to as the balanced design in the current study. At cutting speed, depth of cut and feed of 196.8 m/min, 0.93 mm 0.14 mm/rev, respectively, it compromised between quality, productivity, and process economics, leading to surface roughness of 0.419 μm, material removal rate of 26131.6 mm^3/min and machining power of 4.04 kW. The proposed design was validated against four confirmatory experiments and showed no more than a 7% deviation. The work presented in this study is a novel step towards flexible, adaptive approaches that are not limited to a particular application or set of requirements. Such approaches are essential for the current era of smart, sustainable customer-driven manufacturing. In the future, this work can be extended to include other responses, such as an upgraded cost model where both tool wear and tool initial cost are taken into consideration. These and other extra responses will improve and prove the capability of the proposed model to represent the process. Besides, more measurements as tool chatter, cutting temperature, etc. could be considered in the future while testing different wiper geometries.

REFERENCES

[1] H. A. Hegab, B. Darras, and H. A. Kishawy, "Towards sustainability assessment of machining processes," *J. Cleaner Prod.*, vol. 170, pp. 694–703, Jan. 2018, doi: 10.1016/j.jclepro.2017.09.197.

[2] H. Kishawy, H. Hegab, and E. Saad, "Design for sustainable manufacturing: Approach, implementation, and assessment," *Sustainability*, vol. 10, no. 10, p. 3604, Oct. 2018, doi: 10.3390/su10103604.

[3] H. A. Kishawy, N. S. Reddy, A. Ghandehariun, and H. M. Abdelmoneam, "On a novel solid lubricant–coated cutting tool: Experimental investigation and finite element simulations," *Proc. Inst. Mech. Eng., B, J. Eng. Manuf.*, vol. 229, no. 11, pp. 1893–1899, Nov. 2015, doi: 10.1177/0954405414543482.

[4] G. S. Fox-Rabinovich, K. Yamamoto, B. D. Beake, A. I. Kovalev, M. H. Aguirre, S. C. Veldhuis, G. K. Dosbaeva, D. L. Wainstein, A. Biksa, and A. Rashkovskiy, "Emergent behavior of nano-multilayered coatings during dry high-speed machining of hardened tool steels," *Surf. Coat. Technol.*, vol. 204, nos. 21–22, pp. 3425–3435, Aug. 2010, doi: 10.1016/j.surfcoat.2010.04.002.

[5] S. K. Mishra, S. Ghosh, and S. Aravindan, "Machining performance evaluation of Ti6Al4V alloy with laser textured tools under MQL and nano-MQL environments," *J. Manuf. Processes*, vol. 53, pp. 174–189, May 2020, doi: 10.1016/j.jmapro.2020.02.014.

[6] I. Cascón, J. A. Sarasua, and A. Elkaseer, "Tailored chip breaker development for polycrystalline diamond inserts: FEM-based design and validation," *Appl. Sci.*, vol. 9, no. 19, p. 4117, Oct. 2019, doi: 10.3390/app9194117.

[7] H. A. Kishawy, A. M. Shawky, and M. A. Elbestawi, "Assessment of self-propelled rotating tools during high speed milling," in *Proc. SME 4th Int. Mach. Grinding Conf.*, 2001, pp. 1–11.

[8] H. A. Kishawy, L. Li, and A. El-Wahab, "Prediction of chip flow direction during machining with self-propelled rotary tools," *Int. J. Mach. Tools Manuf.*, vol. 46, pp. 1680–1688, Oct. 2006, doi: 10.1016/j.ijmachtools.2005.06.006.

[9] H. Hegab, "Towards sustainable machining of difficult-to-cut materials using nano-cutting fluids," Fac. Eng. Appl. Sci., Univ. Ontario Inst. Technol., Oshawa, ON, Canada, 2018.

[10] H. Hegab, U. Umer, M. Soliman, and H. A. Kishawy, "Effects of nano-cutting fluids on tool performance and chip morphology during machining Inconel 718," *Int. J. Adv. Manuf. Technol.*, vol. 96, pp. 3449–3458, Mar. 2018, doi: 10.1007/s00170-018-1825-0.
[11] M. Jamil, A. M. Khan, H. Hegab, L. Gong, M. Mia, M. K. Gupta, and N. He, "Effects of hybrid Al_2O_3-CNT nanofluids and cryogenic cooling on machining of Ti-6Al-4V," *Int. J. Adv. Manuf. Technol.*, vol. 102, pp. 3895–3909, Mar. 2019, doi: 10.1007/s00170-019-03485-9.
[12] N. Hanenkamp, S. Amon, and D. Gross, "Hybrid supply system for conventional and CO_2/MQL-based cryogenic cooling," in *Proc. 8th CIRP Conf. High Perform. Cutting (HPC)*, vol. 77, 2018, pp. 219–222, doi: 10.1016/j.procir.2018.08.293.
[13] A. T. Abbas, M. E. Rayes, M. Luqman, N. Naeim, H. Hegab, and A. Elkaseer, "On the assessment of surface quality and productivity aspects in precision hard turning of AISI 4340 steel alloy: Relative performance of wiper vs. Conventional inserts," *Materials*, vol. 13, no. 9, p. 2036, 2020, doi: 10.3390/ma13092036.
[14] D. M. D'Addona and S. J. Raykar, "Analysis of surface roughness in hard turning using wiper insert geometry," in *Proc. 48th CIRP Conf. Manuf. Syst. Res. Innov. Manuf., Key Enabling Technol. Factories Future*, vol. 41, 2016, pp. 841–846, doi: 10.1016/j.procir.2015.12.087.
[15] W. Grzesik and T. Wanat, "Surface finish generated in hard turning of quenched alloy steel parts using conventional and wiper ceramic inserts," *Int. J. Mach. Tools Manuf.*, vol. 46, pp. 1988–1995, Dec. 2006, doi: 10.1016/j.ijmachtools.2006.01.009.
[16] A. Elkaseer, A. Abdelaziz, M. Saber, and A. Nassef, "FEM-based study of precision hard turning of stainless steel 316L," *Materials*, vol. 12, no. 16, p. 2522, Aug. 2019, doi: 10.3390/ma12162522.
[17] M. Elbah, M. A. Yallese, H. Aouici, T. Mabrouki, and J.-F. Rigal, "Comparative assessment of wiper and conventional ceramic tools on surface roughness in hard turning AISI 4140 steel," *Measurement*, vol. 46, no. 9, pp. 3041–3056, Nov. 2013, doi: 10.1016/j.measurement.2013.06.018.
[18] A. P. Paiva, P. H. Campos, J. R. Ferreira, L. G. D. Lopes, E. J. Paiva, and P. P. Balestrassi, "A multivariate robust parameter design approach for optimization of AISI 52100 hardened steel turning with wiper mixed ceramic tool," *Int. J. Refractory Met. Hard Mater.*, vol. 30, no. 1, pp. 152–163, Jan. 2012, doi: 10.1016/j.ijrmhm.2011.08.001.
[19] K. V. Subbaiah, C. Raju, R. S. Pawade, and C. Suresh, "Machinability investigation with wiper ceramic insert and optimization during the hard turning of AISI 4340 steel," *Mater. Today, Proc.*, vol. 18, pp. 445–454, 2019, doi: 10.1016/j.matpr.2019.06.300.
[20] V. N. Gaitonde, S. R. Karnik, L. Figueira, and J. P. Davim, "Performance comparison of conventional and wiper ceramic inserts in hard turning through artificial neural network modeling," *Int. J. Adv. Manuf. Technol.*, vol. 52, nos. 1–4, pp. 101–114, Jan. 2011, doi: 10.1007/s00170-010-2714-3.
[21] U. A. Dabade, S. S. Joshi, and N. Ramakrishnan, "Analysis of surface roughness and chip cross-sectional area while machining with self-propelled round inserts milling cutter," *J. Mater. Process. Technol.*, vol. 132, pp. 305–312, Jan. 2003, doi: 10.1016/S0924-0136(02)00949-4.
[22] G. Basmaci and M. Ay, "Optimization of cutting parameters, condition and geometry in turning AISI 316L stainless steel using the grey-based Taguchi method," *Acta Phys. Polonica A*, vol. 131, no. 3, pp. 354–359, Mar. 2017, doi: 10.12693/APhysPolA.131.354.
[23] M. Ay, "Optimisation of machining parameters in turning AISI 304L stainless steel by the grey-based Taguchi method," *Acta Phys. Polonica A*, vol. 131, no. 3, pp. 349–354, Mar. 2017, doi: 10.12693/APhysPolA.131.349.
[24] K. V. Subbaiah, C. Raju, and C. Suresh, "Comparative assessment of cutting inserts and optimization during hard turning: Taguchi-based grey relational analysis," in *Proc. IOP Conf. Ser. Mater. Sci. Eng.*, vol. 225, 2017, pp. 1–9, doi: 10.1088/1757-899X/225/1/012165.
[25] P. H. S. Campos, G. Belinato, T. I. Paula, M. de Oliveira-Abans, J. R. Ferreira, A. P. Paiva, and P. P. Balestrassi, "Multivariate mean square error for the multiobjective optimization of AISI 52100 hardened steel turning with wiper ceramic inserts tool: A comparative study," *J. Brazilian Soc. Mech. Sci. Eng.*, vol. 39, no. 10, pp. 4021–4036, Oct. 2017, doi: 10.1007/s40430-017-0841-6.
[26] T. Zhang, O. Owodunni, and J. Gao, "Scenarios in multi-objective optimisation of process parameters for sustainable machining," in *Proc. 12th Global Conf. Sustain. Manuf.–Emerg. Potentials*, vol. 26, pp. 373–378, 2015, doi: 10.1016/j.procir.2014.07.186.
[27] S. A. Bagaber and A. R. Yusoff, "Multi-objective optimization of cutting parameters to minimize power consumption in dry turning of stainless steel 316," *J. Cleaner Prod.*, vol. 157, pp. 30–46, Jul. 2017, doi: 10.1016/j.jclepro.2017.03.231.
[28] S. A. Bagaber and A. R. Yusoff, "Energy and cost integration for multi-objective optimisation in a sustainable turning process," *Measurement*, vol. 136, pp. 795–810, Mar. 2019, doi: 10.1016/j.measurement.2018.12.096.
[29] D.-H. Lee, K.-J. Kim, and M. Köksalan, "A posterior preference articulation approach to multiresponse surface optimization," *Eur. J. Oper. Res.*, vol. 210, no. 2, pp. 301–309, Apr. 2011, doi: 10.1016/j.ejor.2010.09.032.
[30] D.-H. Lee and K. J. Kim, "A review on posterior and interactive solution selection methods to multiresponse surface optimization," *J. Qual.*, vol. 18, no. 4, pp. 279–301, 2011.
[31] B. Pytlak, "Multicriteria optimization of hard turning operation of the hardened 18HGT steel," *Int. J. Adv. Manuf. Technol.*, vol. 49, nos. 1–4, pp. 305–312, Jul. 2010, doi: 10.1007/s00170-009-2375-2.
[32] D.-H. Lee, I.-J. Jeong, and K.-J. Kim, "A desirability function method for optimizing mean and variability of multiple responses using a posterior preference articulation approach," *Qual. Rel. Eng. Int.*, vol. 34, no. 3, pp. 360–376, Apr. 2018, doi: 10.1002/qre.2258.
[33] D.-H. Lee and I.-J. Jeong, "IP-MRSO: An iterative posterior preference articulation method to multiple response surface optimization," *Qual. Rel. Eng. Int.*, vol. 33, no. 8, pp. 1813–1826, Dec. 2017, doi: 10.1002/qre.2145.
[34] M. Abubakr, A. T. Abbas, I. Tomaz, M. S. Soliman, M. Luqman, and H. Hegab, "Sustainable and smart manufacturing: An integrated approach," *Sustainability*, vol. 12, no. 6, p. 2280, Mar. 2020, doi: 10.3390/su12062280.
[35] S. Wang, J. Wan, D. Li, and C. Zhang, "Implementing smart factory of industrie 4.0: An outlook," *Int. J. Distrib. Sensor Netw.*, vol. 12, no. 1, Jan. 2016, Art. no. 3159805, doi: 10.1155/2016/3159805.
[36] M. A. Hassan, A. Khalil, S. Kaseb, and M. A. Kassem, "Independent models for estimation of daily global solar radiation: A review and a case study," *Renew. Sustain. Energy Rev.*, vol. 82, pp. 1565–1575, Feb. 2018, doi: 10.1016/j.rser.2017.07.002.
[37] M. Abubakr, H. Amein, B. M. Akoush, M. M. El-Bakry, and M. A. Hassan, "An intuitive framework for optimizing energetic and exergetic performances of parabolic trough solar collectors operating with nanofluids," *Renew. Energy*, vol. 157, pp. 130–149, Sep. 2020, doi: 10.1016/j.renene.2020.04.160.
[38] M. A. Hassan and D. Banerjee, "A soft computing approach for estimating the specific heat capacity of molten salt-based nanofluids," *J. Mol. Liquids*, vol. 281, pp. 365–375, May 2019, doi: 10.1016/j.molliq.2019.02.106.
[39] E. Ahmadloo and S. Azizi, "Prediction of thermal conductivity of various nanofluids using artificial neural network," *Int. Commun. Heat Mass Transf.*, vol. 74, pp. 69–75, May 2016, doi: 10.1016/j.icheatmasstransfer.2016.03.008.
[40] T. Ghosh and K. Martinsen, "Generalized approach for multi-response machining process optimization using machine learning and evolutionary algorithms," *Eng. Sci. Technol., Int. J.*, vol. 23, no. 3, pp. 650–663, Jun. 2020, doi: 10.1016/j.jestch.2019.09.003.
[41] C. Divya, L. S. Raju, and B. Singaravel, "A Review of TOPSIS method for multi criteria optimization in manufacturing environment," in *Proc. Int. Conf. Innov. Mod. Sci. Technol.*, 2020, pp. 719–727, doi: 10.1007/978-3-030-42363-6_84.
[42] K. Deb, A. Pratap, S. Agarwal, and T. Meyarivan, "A fast and elitist multiobjective genetic algorithm: NSGA-II," *IEEE Trans. Evol. Comput.*, vol. 6, no. 2, pp. 182–197, Apr. 2002, doi: 10.1109/4235.996017.
[43] R. L. Haupt and S. E. Haupt, *Practical Genetic Algorithms*. Hoboken, NJ, USA: Wiley, 2003, doi: 10.1002/0471671746.
[44] S. Cheng, Y. Shi, and Q. Qin, "On the performance metrics of multiobjective optimization," in *Advances in Swarm Intelligence. ICSI* (Lecture Notes in Computer Science), vol. 7331, Y. Tan, Y. Shi, and Z. Ji, Eds. Berlin, Germany: Springer, 2012, doi: 10.1007/978-3-642-30976-2_61.
[45] K. Deb, *Multi-Objective Optimization Using Evolutionary Algorithms*. Hoboken, NJ, USA: Wiley, 2001.
[46] M. H. Esfe, M. H. Hajmohammad, N. Sina, and M. Afrand, "Optimization of thermophysical properties of Al_2O3/water-EG (80:20) nanofluids by NSGA-II," *Phys. E, Low-Dimensional Syst. Nanostruct.*, vol. 103, pp. 264–272, Sep. 2018, doi: 10.1016/j.physe.2018.05.031.
[47] W. Knight and G. Boothroyd, *Fundamentals of Metal Machining and Machine Tools*. Boca Raton, FL, USA: CRC Press, 2005, doi: 10.1201/9780429114243.
[48] Z. Q. Liu, P. Zhang, P. Guo, and X. Ai, "Surface roughness in high feed turning with wiper insert," *Key Eng. Mater.*, vols. 375–376, pp. 406–410, Mar. 2008.
[49] L. Jiang and D. Wang, "Finite-element-analysis of the effect of different wiper tool edge geometries during the hard turning of AISI 4340 steel," *Simul. Model. Pract. Theory*, vol. 94, pp. 250–263, Jul. 2019, doi: 10.1016/j.simpat.2019.03.006.

[50] V. N. Gaitonde, S. R. Karnik, L. Figueira, and J. P. Davim, "Machinability investigations in hard turning of AISI d2 cold work tool steel with conventional and wiper ceramic inserts," *Int. J. Refractory Met. Hard Mater.*, vol. 27, no. 4, pp. 754–763, Jul. 2009, doi: 10.1016/j.ijrmhm.2008.12.007.
[51] J. P. Davim and L. Figueira, "Comparative evaluation of conventional and wiper ceramic tools on cutting forces, surface roughness, and tool wear in hard turning AISI d2 steel," *Proc. Inst. Mech. Eng., B, J. Eng. Manuf.*, vol. 221, no. 4, pp. 625–633, Apr. 2007, doi: 10.1243/09544054JEM762.
[52] G. T. Smith, *Cutting Tool Technology*. London, U.K.: Springer, 2008, doi: 10.1007/978-1-84800-205-0.
[53] J. A. Williams, "Fundamentals of metal cutting and machine tools," *Mater. Des.*, vol. 9, no. 5, p. 303, 1988, doi: 10.1016/0261-3069(88)90021-0.

ADEL TAHA ABBAS is a Professor with the Department of Mechanical Engineering, King Saud University. His current research interest includes the multi-criteria optimization of machining parameters using artificial intelligence.

MOHAMED ABUBAKR is currently pursuing the M.Sc. degree with the Faculty of Engineering, Cairo University. He is a Research Assistant with The American University in Cairo. His research interests include engineering systems modeling and optimization.

AHMED ELKASEER has more than 15 years' experience of research in experimental, modeling, simulation, and optimization-based studies of advanced manufacturing processes, with a recent emphasis on additive manufacturing and Industry 4.0 applications. He is a Senior Research Associate with the Karlsruhe Institute of Technology.

MAGDY M. EL RAYES is a Professor of mechanical engineering with King Saud University. He is specialized in the fields of materials science and manufacturing processes. His main research interests include severe plastic deformation processes and materials characterization in a variety of manufacturing applications.

MONIS LUQMAN MOHAMMED is currently pursuing the Ph.D. degree in mechanical engineering with King Saud University, Saudi Arabia. His research interests include nanomaterials, biocompatible polymers, ceramics, tissue engineering, powder metallurgy, and biomaterials.

HUSSIEN HEGAB is an Assistant Professor with the Department of Mechanical Design and Production Engineering, Cairo University, Egypt. His research interest includes promoting sustainable machining of hard-to-cut materials with a special focus on green cooling strategies.